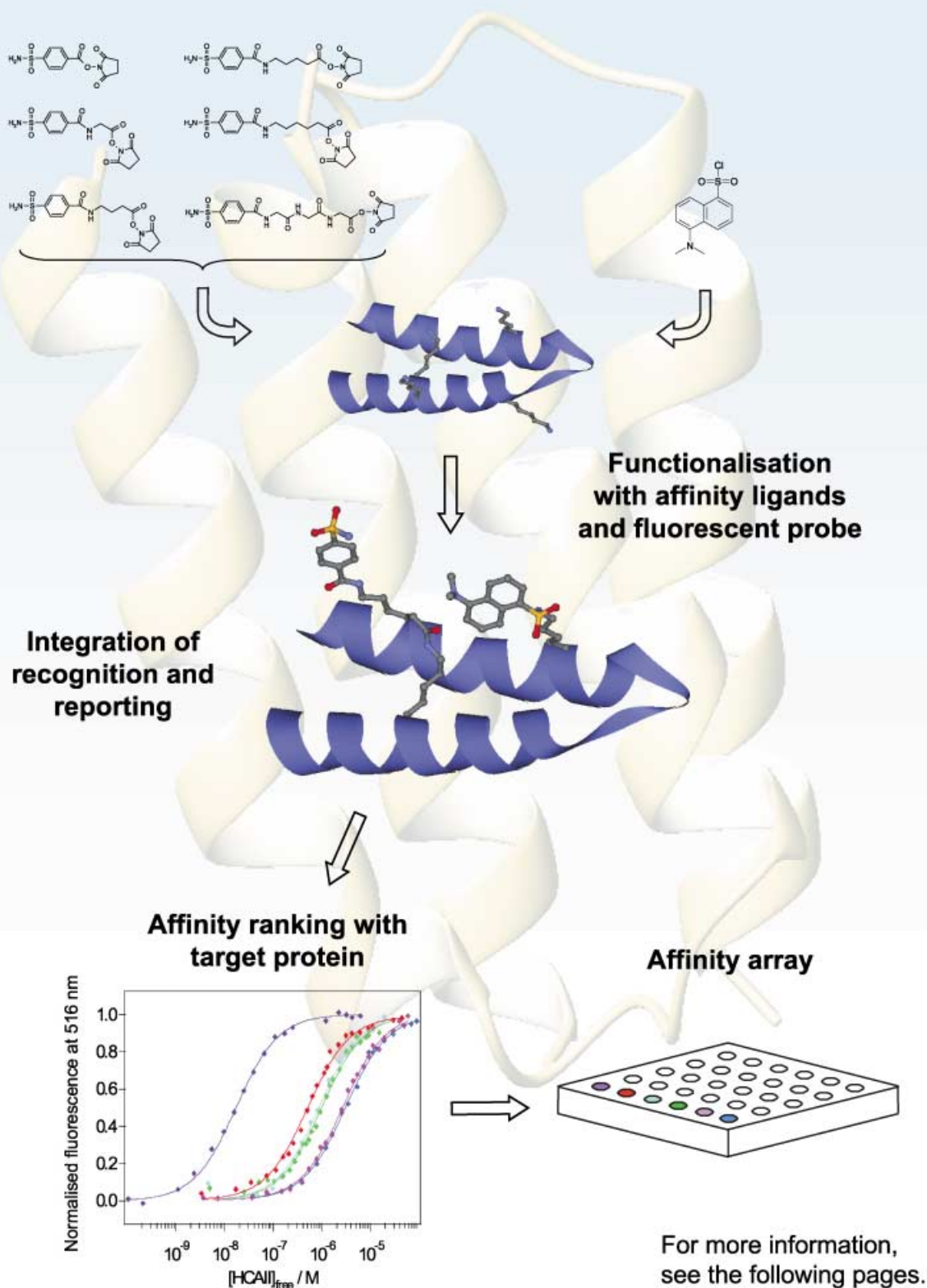


## Self-functionalising helix-loop-helix polypeptides for microarray applications



# A Versatile Polypeptide Platform for Integrated Recognition and Reporting: Affinity Arrays for Protein–Ligand Interaction Analysis

Karin Enander,<sup>[a]</sup> Gunnar T. Dolphin,<sup>[a]</sup> Bo Liedberg,<sup>[b]</sup> Ingemar Lundström,<sup>[c]</sup> and Lars Baltzer\*<sup>[a]</sup>

**Abstract:** A molecular platform for protein detection and quantification is reported in which recognition has been integrated with direct monitoring of target-protein binding. The platform is based on a versatile 42-residue helix–loop–helix polypeptide that dimerizes to form four-helix bundles and allows site-selective modification with recognition and reporter elements on the side chains of individually addressable lysine residues. The well-characterized interaction between the model target-protein carbonic anhydrase and its inhibitor benzenesulfonamide was used for a proof-of-concept demonstration.

An affinity array was designed where benzenesulfonamide derivatives with aliphatic or oligoglycine spacers and a fluorescent dansyl reporter group were introduced into the scaffold. The affinities of the array members for human carbonic anhydrase II (HCAII) were determined by titration with the target protein and were found to be highly affected by the properties of the spacers (dissociation constant  $K_d = 0.02\text{--}3\ \mu\text{M}$ ).

**Keywords:** affinity arrays • biosensors • fluorescence • peptide scaffolds • protein chips

The affinity of HCAII for acetazolamide ( $K_d = 4\ \text{nM}$ ) was determined in a competition experiment with one of the benzenesulfonamide array members to address the possibility of screening substance libraries for new target-protein binders. Also, successful affinity discrimination between different carbonic anhydrase isozymes highlighted the possibility of performing future isoform-expression profiling. Our platform is predicted to become a flexible tool for a variety of biosensor and protein-microarray applications within biochemistry, diagnostics and pharmaceutical chemistry.

## Introduction

The development of protein-chip technology, where immobilized capture molecules are used for parallel detection and quantification of proteins in a high-throughput manner, is driven by the current need for rapid large-scale analysis of protein function and expression.<sup>[1–3]</sup> One of the most impor-

tant aspects of protein-chip design is the choice of capture molecules. We and others<sup>[4–9]</sup> have identified polypeptides as attractive candidates, as they are robust and easily synthesized by well-established methods and because of the huge chemical diversity that can be generated in a short time with modest synthetic cost and effort. The amino acid sequence can be varied over a wide range to provide access to a variety of scaffold structures, and highly specific recognition sites and reporter groups can be introduced postsynthetically by orthogonal strategies on the solid phase. In our laboratory, de novo designed 42 amino acid helix–loop–helix polypeptides that undergo pH-controlled site-selective self-functionalization with activated esters have been extensively explored.<sup>[10–12]</sup> Function is intimately coupled to structure, as the fold governs the reactivity of the functionalization sites through  $pK_a$  depression of lysine side chains in the hydrophobic core and through control of the reactivity of His–Lys pairs. In these scaffolds, a number of lysine residues can be individually addressed in aqueous solution in an automated fashion without the need for protecting-group chemistry or intermediate steps of purification. The fold also provides directionality and well-defined distances between amino acid residues. Polypeptide scaffolds designed according to these principles constitute powerful tools for the construction of,

[a] Dr. K. Enander, Dr. G. T. Dolphin, Prof. L. Baltzer  
Division of Chemistry  
Department of Physics and Measurement Technology  
Biology and Chemistry  
Linköping University, 58183 Linköping (Sweden)  
Fax: (+46) 13-122587  
E-mail: Lars.Baltzer@ifm.liu.se

[b] Prof. B. Liedberg  
Division of Sensor Science  
Department of Physics and Measurement Technology  
Biology and Chemistry  
Linköping University, 58183 Linköping (Sweden)

[c] Prof. I. Lundström  
Division of Applied Physics  
Department of Physics and Measurement Technology  
Biology and Chemistry  
Linköping University, 58183 Linköping (Sweden)

for example, model glycoproteins<sup>[13,14]</sup> and complex receptors (L. Baltzer et al., unpublished data).

We have previously reported on the design of a functional biosensor unit based on a helix–loop–helix polypeptide that dimerises in solution to form a four-helix bundle.<sup>[15]</sup> A biosensor provides identification and quantification of a target substance (analyte) by coupling a highly specific biomolecular recognition event to changes in physical signals.<sup>[16]</sup> So-called affinity biosensors, where the detection signal is a direct result of analyte binding, frequently employ an optical transduction mechanism. An attractive approach involves fluorescence detection, where the events of recognition and signalling are integrated by attaching a fluorescent reporter group to the recognition element in a fashion that allows the reporter to respond to analyte binding.<sup>[17]</sup>

Microarrays of capture molecules may provide traditional biosensor signals as well as pattern analysis. We focus on the design of a flexible molecular platform from which to build integrated units of recognition and reporting for the analysis, on a chip or in solution, of a variety of protein–ligand systems in an array format. The traditional labelling of the analyte is avoided since reporting is provided by the capture agent. In a previous communication, the well-characterized interaction between the target-protein carbonic anhydrase (CA) and a benzenesulfonamide ligand was selected for a proof-of-concept demonstration.<sup>[15]</sup> The fluorescence of a peptide modified with a benzenesulfonamide derivative and a fluorescent probe was monitored as a function of CA concentration and the dissociation constant  $K_d$  was determined. Here, we report on the design of a six-membered polypeptide affinity array for CA, constructed by varying the spacer of the benzenesulfonamide derivative. Interaction studies of the highest-affinity member with different CA isozymes address the possibility of protein-expression profiling in a future diagnostic application, while competition experiments with the inhibitor acetazolamide show the applicability of this technology to screening substance libraries for candidate drugs.

## Results

**Scaffold design:** A folded polypeptide was chosen as the basic building block for the construction of general biosensor molecules, to provide well-defined distances and geometries between the amino acid side chains. The 42-residue polypeptide SA-42 has been shown previously by NMR spectroscopy, circular dichroism spectroscopy and analytical ultracentrifugation to form a helix–loop–helix motif that dimerises in solution to form a four-helix bundle.<sup>[18,19]</sup> The design of KE2 (Figure 1 a) was based on the structure of the 42-residue helix–loop–helix polypeptide LA-42b,<sup>[13]</sup> a daughter sequence of SA-42 that contains five sites for acylation on the side chains of lysine and ornithine residues. The versatility of LA-42b as a scaffold was demonstrated by the sequential and site-selective incorporation of three substituents into the protein scaffold in aqueous solution without intermediate purification.<sup>[20]</sup> In KE2, 36 out of the 42 amino acids of LA-42b were conserved. Lysine residues in posi-

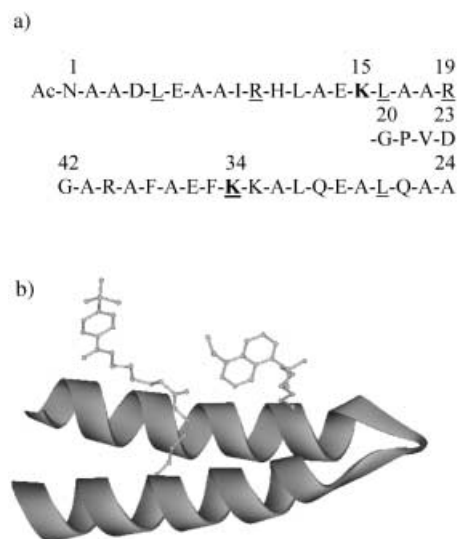


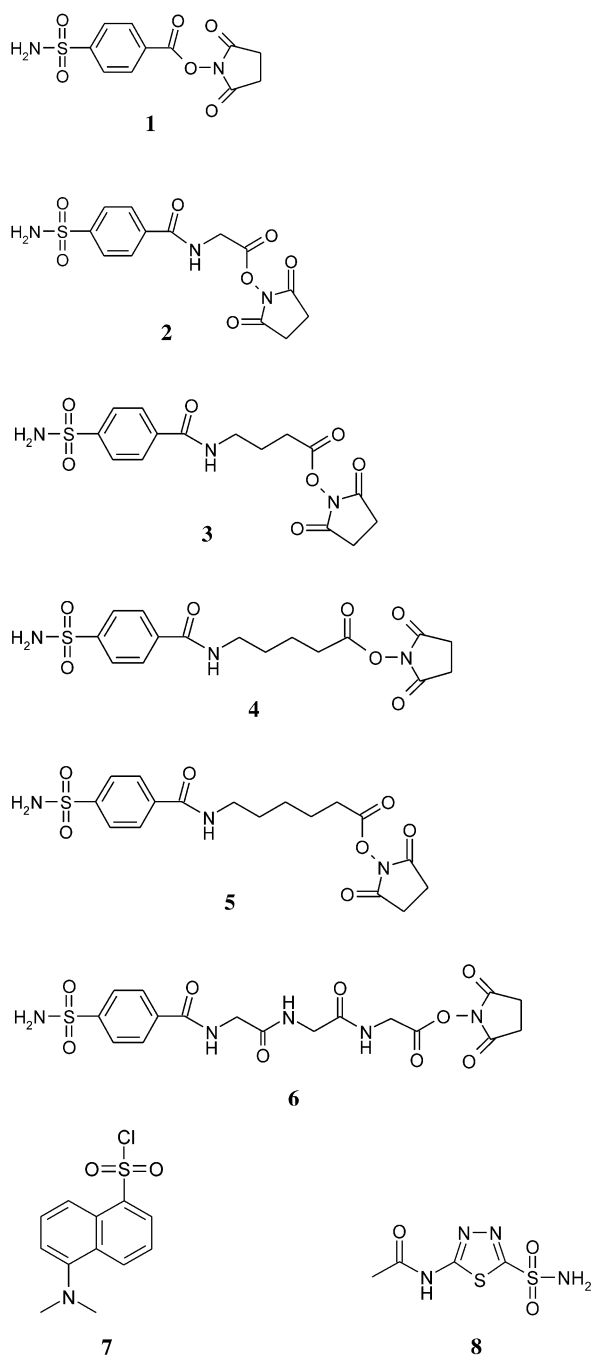
Figure 1. a) The amino acid sequence of KE2, where lysine residues in bold represent addressable sites for modification. The amino terminal was acetylated. Residues that differ from those in the template peptide LA-42b<sup>[13]</sup> are underlined. The one letter code for amino acids is used: A = Ala, D = Asp, E = Glu, F = Phe, G = Gly, H = His, I = Ile, K = Lys, L = Leu, N = Asn, P = Pro, Q = Gln, R = Arg, V = Val. b) Cartoon of KE2-D(15)-5 based on the crystal structure of the four-helix-bundle rop protein (PDB entry code: 1ROP).<sup>[45]</sup> The rop helices were shortened, the amino acids were changed to those of KE2 and the dansyl probe **7** and benzenesulfonamide **5** were attached in positions 15 and 34, respectively (Sybyl, Tripos Inc.). The polypeptide is folded only when dimerized, but for reasons of clarity the monomer is shown.

tions 15 and 34 were targeted for postsynthetic modifications to enhance the probability that the analyte-binding event would result in interactions between the reporter group and the analyte because of the proximity and similar directionality of the incorporated groups in the folded state. Orthogonal protecting-group chemistry was used for the functionalization of position 15, while position 34 was acylated in aqueous solution.

**Choice of model system:** In the development of a general biosensor platform, the availability of a well-characterized model system is crucial for showing proof-of-concept and for the elucidation of the fundamental characteristics of the scaffold. The interaction between CA and benzenesulfonamide was selected in the development of a KE2-based biosensor molecule.<sup>[15]</sup> Human carbonic anhydrase II (HCAII), the most studied of several CA isoforms, is a globular, monomeric enzyme that catalyses the reversible hydration of carbon dioxide. The enzymatic activity is mediated by a tetrahedrally coordinated zinc ion, located in a cavity that is 15-Å deep, where it is ligated by three histidine residues.<sup>[21]</sup> Aromatic and heterocyclic sulfonamides are powerful inhibitors of HCAII<sup>[22,23]</sup> and inhibition is caused by competitive coordination of the ionized sulfonamide nitrogen atom to the zinc ion.<sup>[24]</sup> The interactions between HCAII (and the bovine equivalent BCAII) and a wide range of benzenesulfonamide derivatives have been thoroughly characterized in the quest for high-affinity inhibitors,<sup>[25–31]</sup> and the availability of structural data for enzyme–benzenesulfonamide com-

plexes<sup>[30,32]</sup> as well as the monovalent character of the interaction made it an attractive model system for the evaluation of the polypeptide-based biosensor platform.

5-Dimethylaminonaphthalene-1-sulfonyl chloride (dansyl chloride, **7**, Scheme 1)<sup>[33]</sup> was chosen for reporting because when it reacts with amines it forms fluorescent probes characterized by environmentally sensitive fluorescence quantum yields and emission maxima (excitation  $\lambda_{\text{max}} = 335$  nm in methanol).<sup>[34,35]</sup> Preliminary data with dansyl or 7-nitrobenzo-2-oxa-1,3-diazole (NBD) probes in position 15 of KE2 indicated that the dansyl signal in that position was influenced



Scheme 1. Structures of the six benzenesulfonamide derivatives used in the affinity series (**1–6**), dansyl chloride (**7**) and the CA inhibitor acetazolamide (**8**).

to a larger extent by HCAII binding than the signal from NBD (data not shown).

**Design of an affinity array:** Six derivatives of 4-carboxybenzenesulfonamide (**1–6**, Scheme 1) were synthesized and incorporated into the KE2 polypeptide scaffold to form a six-membered affinity array for HCAII. Benzenesulfonamides substituted in the *para* position with alkyl, oligo(ethylene glycol) or oligopeptide residues are known to bind tighter to CA than  $\text{H}_2\text{NO}_2\text{SC}_6\text{H}_5$  does, due to interactions with a hydrophobic patch in the enzyme binding cleft.<sup>[26–29,31]</sup> A gradual increase in the number of methylene groups in the alkyl chain is accompanied by a decrease in the  $K_d$  value,<sup>[25,29]</sup> but there is no such correlation when extending the substituent with more than one ethylene glycol or glycine group.<sup>[28]</sup> We therefore selected a series of aliphatic substituents containing between one and five methylene groups (**2–5**) in the design of the array, expecting steric constraints caused by the polypeptide scaffold as well as binding-energy contributions from the spacer methylene groups to influence the affinity. Inspection of the crystal structure of HCAII complexed with  $\text{H}_2\text{NO}_2\text{SC}_6\text{H}_4\text{CONH}(\text{CH}_2\text{CH}_2\text{O})_2\text{CH}_2\text{CH}_2\text{NH}_2$  (PDB entry 1CNX)<sup>[30]</sup> suggested that KE2 functionalized with **5** in position 34 (and possibly some of the ligands with shorter spacers as well) should be able to reach into the pocket without distorting the polypeptide structure. A triglycine derivative, **6**, was included in the array to allow a comparison between the hydrophobic spacer provided by **5** and a less flexible, more polar one of similar length. The carboxybenzenesulfonamide derivative **1** was also included.

#### Peptide synthesis, functionalization and structural characterization

The polypeptide KE2 was synthesized on the solid phase and a dansyl probe (D) was introduced after selective deprotection of the amine group on the side chain of Lys15 to form KE2-D(15). The peptide was cleaved from the resin by 95% trifluoroacetic acid, purified by reversed-phase HPLC and identified from the MALDI-TOF mass spectrometry. The benzenesulfonamide ligands **1–6** were incorporated on the side chain of Lys34 by reaction with KE2-D(15) in aqueous solution at pH 8.0 to form the peptides KE2-D(15)-X (X = **1–6**). (KE2-D(15) corresponds to KE2-P in earlier work<sup>[15]</sup> and KE2-D(15)-**5** corresponds to KE2-PL.) The purified peptides were identified by MALDI-TOF mass analysis. Due to the much higher reactivity of Orn34 than of Lys33 in peptides derived from LA-42b,<sup>[11]</sup> monomodification of KE2 was assumed to have taken place exclusively on the side chain of Lys34. A cartoon of KE2-D(15)-**5** is shown in Figure 1b to illustrate the relative positions of the incorporated ligands.

The secondary structure content of KE2-D(15) and KE2-D(15)-X (X = **1–6**) in 100 mM sodium phosphate at pH 7.4 and at the concentration used for fluorescence spectroscopy studies was determined by circular dichroism spectroscopy (Table 1). Helical proteins show a characteristic signature with minima at 208 and 222 nm and all peptides reported here were found to exhibit a high helical content with mean residue ellipticities at 222 nm,  $[\theta]_{222}$ , in the range of  $-18000$  to  $-20000$  deg cm<sup>2</sup> dmol<sup>-1</sup>. The corresponding mean residue

Table 1. The mean residue ellipticities at 222 nm of KE2, KE2-D(15) and KE2-D(15)-X (X=1–6).<sup>[a]</sup>

Peptide	Mean residue ellipticity [ $\theta$ ] <sub>222</sub> [deg cm <sup>2</sup> dmol <sup>-1</sup> ]
KE2	-14600
KE2-D(15)	-19800
KE2-D(15)-1	-19600
KE2-D(15)-2	-19400
KE2-D(15)-3	-19800
KE2-D(15)-4	-18600
KE2-D(15)-5	-18200
KE2-D(15)-6	-20000

[a] Measured at concentrations of 1  $\mu\text{M}$  (or 0.8  $\mu\text{M}$  in the case of KE2-D(15)-5) in 100 mM sodium phosphate at pH 7.4. The experimental error was estimated to be  $\pm 1000$  deg cm<sup>2</sup> dmol<sup>-1</sup>.

ellipticity of KE2 was only  $-14600$  deg cm<sup>2</sup> dmol<sup>-1</sup> and the incorporation of substituents thus stabilized the folded structure, in agreement with what was previously observed upon glycosylation of LA-42b.<sup>[13,36]</sup> This effect might be due to the neutralization of the positive charge of the side chain of Lys34 upon functionalization, but dansyl and benzenesulfonamide groups may also stabilise the peptide through interactions within the hydrophobic core. The KE2 scaffold is a more stable four-helix bundle than LA-42b at low micromolar concentrations, probably due to differences in the amino acids that build up the peptide core<sup>[13]</sup> resulting in better hydrophobic packing in KE2.

**Affinity studies:** The biosensing ability of KE2-D(15)-5 has been demonstrated previously and its affinity for HCAII was 0.02  $\mu\text{M}$ .<sup>[15]</sup> The basis for biosensing was the fluorescence-intensity increase of the dansyl probe upon peptide binding to HCAII. Here, the affinities of KE2-D(15)-X (X=1–6) were determined fluorometrically at pH 7.4 and KE2-D(15) was included as a negative control. Samples of 1  $\mu\text{M}$  peptide (or 0.8  $\mu\text{M}$  in the case of KE2-D(15)-5) were excited at 335 nm. Upon titration with HCAII (5 nM–90  $\mu\text{M}$ ), the fluorescence intensity increased. The maximum enhancements of KE2-D(15)-X (X=1–6) varied between 90% (KE2-D(15)-1) and 225% (KE2-D(15)-5, Figure 2). No enhancement was obtained for KE2-D(15). Only small effects

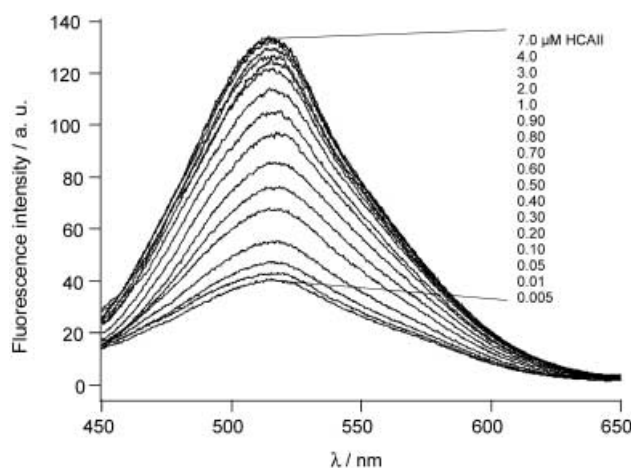


Figure 2. Fluorescence spectra of 0.8  $\mu\text{M}$  KE2-D(15)-5 as a function of HCAII concentration. The intensity maximum was at 516 nm.

on the Stokes' shifts were observed and the intensity maximum in the absence of HCAII was 516–518 nm. All peptides except KE2-D(15)-5 displayed a slight blue shift of  $\approx 5$  nm when bound to HCAII, a result that indicates a less polar environment of the probe in the bound peptide than in the unbound state. The affinities were determined by plotting the fluorescence intensity at 516 nm versus the total concentration of HCAII and fitting an equation describing the dissociation of a bimolecular complex to the experimental results (Figure 3). The  $K_d$  value was confirmed to be 0.02  $\mu\text{M}$  for the interaction between KE2-D(15)-5 and HCAII, while the affinities of the other peptides were in the range 0.7–3  $\mu\text{M}$  (Table 2). The affinity of KE2-D(15)-4 was measured four times ( $K_d=0.61, 0.77, 0.84$  and 0.85  $\mu\text{M}$ ) and that of KE2-D(15)-2 was measured twice ( $K_d=0.50$  and 0.82  $\mu\text{M}$ ). From this result, the experimental errors were estimated not to exceed  $\pm 20\%$ .

The affinity of  $\text{H}_2\text{NO}_2\text{SC}_6\text{H}_5$  for HCAII is described by a dissociation constant,  $K_d$ , of 1.5  $\mu\text{M}$ ,<sup>[25]</sup> and *para*-substituted

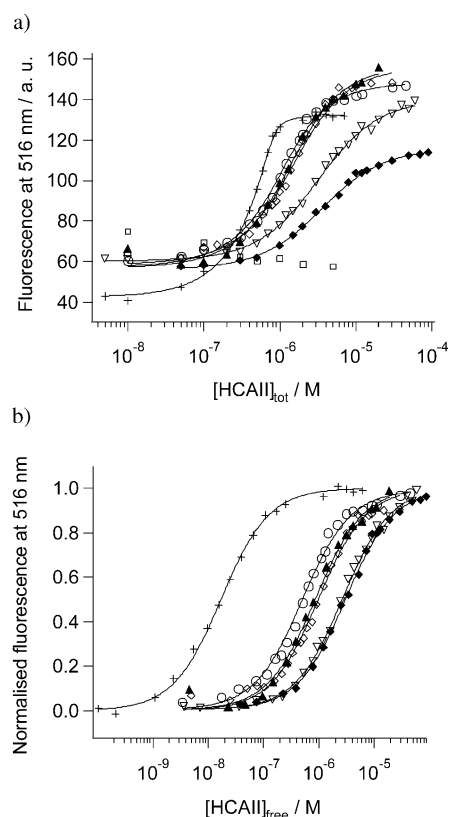


Figure 3. a) Fluorescence intensity at 516 nm of 1  $\mu\text{M}$  peptide (or 0.8  $\mu\text{M}$  in the case of KE2-D(15)-5) as a function of HCAII concentration. All peptides, except the negative control KE2-D(15) ( $\square$ ), display increased intensities upon addition of HCAII. An equation that describes the dissociation of a bimolecular complex was fitted to the experimental data to obtain the  $K_d$  values: KE2-D(15)-1 ( $\blacklozenge$ ,  $K_d=3$   $\mu\text{M}$ ), KE2-D(15)-2 ( $\diamond$ , 1  $\mu\text{M}$ ), KE2-D(15)-3 ( $\circ$ , 0.7  $\mu\text{M}$ ), KE2-D(15)-4 ( $\blacktriangle$ , 0.8  $\mu\text{M}$ ), KE2-D(15)-5 ( $+$ , 0.02  $\mu\text{M}$ ), KE2-D(15)-6 ( $\nabla$ , 3  $\mu\text{M}$ ). Average  $K_d$  values for KE2-D(15)-3 (two measurements) and KE2-D(15)-4 (four measurements) are given, while representative data sets are shown in the figure. Solid lines represent the best fits to the experimental results. b) Binding curves obtained by plotting normalized fluorescence data versus the concentration of free HCAII,  $[\text{HCAII}]_{\text{free}}$ . The concentrations were calculated from the  $K_d$  values.

Table 2. Carbonic anhydrase II affinities for free versus polypeptide-conjugated benzenesulfonamides with aliphatic and oligoglycine substituents or spacers.  $n$  = number of methylene groups. Cited  $K_d$  values for measurements with HCAII and BCAII are included.

Sulfonamide	Protein	$K_d$ [ $\mu\text{M}$ ]				
		$n=1$	$n=2$	$n=3$	$n=4$	$n=5$
$\text{H}_2\text{NO}_2\text{S}(\text{C}_6\text{H}_4)\text{CONH}(\text{CH}_2)_n\text{CONH-KE2-D(15)}$	HCAII	1	nd	0.7 <sup>[a]</sup>	0.8 <sup>[b]</sup>	0.02
$\text{H}_2\text{NO}_2\text{S}(\text{C}_6\text{H}_4)\text{CONH}(\text{CH}_2)_{n-1}\text{CH}_3^{\text{[c]}}$	HCAII	0.08	0.03	0.008	0.0032	0.0018
$\text{H}_2\text{NO}_2\text{S}(\text{C}_6\text{H}_4)\text{CONH}(\text{CH}_2)_{n-1}\text{CH}_3^{\text{[d]}}$	BCAII	nd	0.17	0.038	0.016	nd
$\text{H}_2\text{NO}_2\text{S}(\text{C}_6\text{H}_4)\text{CO}(\text{Gly})_3\text{-KE2-D(15)}$	HCAII	3				
$\text{H}_2\text{NO}_2\text{S}(\text{C}_6\text{H}_4)\text{CO}(\text{Gly})_4\text{OH}^{\text{[e]}}$	HCAII	0.36				

[a] Average of two measurements, see text for details. [b] Average of four measurements, see text for details. [c] From ref. [26]. The affinities were measured in 50 mM tris(hydroxymethyl)aminomethane (Tris)/ $\text{H}_2\text{SO}_4$  (pH 8.0). [d] From ref. [29]. The affinities were measured in 20 mM phosphate buffer (pH 7.5) at 37 °C. [e] From ref. [31]. The affinities were measured at pH 7.5, the buffer used was not stated. nd = not determined.

benzenesulfonamides resembling **2–5** span the affinity range of 80–2 nM<sup>[26]</sup> due to the additional binding energy between the enzyme binding cleft and the hydrophobic substituents. In the peptides reported here lower affinities were observed (1–0.02  $\mu\text{M}$ , Table 2), probably as a result of steric strain caused by contact between HCAII and the scaffold. The dependence of affinity values on the spacer lengths of peptide-linked benzenesulfonamide derivatives was very different from that of similar benzenesulfonamides not coupled to the peptide scaffold. There was virtually no affinity difference between the peptides KE2-D(15)-**2**, KE2-D(15)-**3** and KE2-D(15)-**4**, but a striking effect of a single methylene group was observed when comparing the affinities of KE2-D(15)-**4** and KE2-D(15)-**5**. The nanomolar affinity that arises from cooperativity between zinc-ion coordination and spacer–protein hydrophobic interactions and that is characteristic of benzenesulfonamide ligands with aliphatic substituents when not coupled to a scaffold was only observed with five methylene groups in the spacer. Although this is the most likely explanation, we do not exclude the possibility that other parameters might also influence the binding affinities, for example, interactions between the target protein and the reporter group, the side chain of Lys34 or the side chains of other amino acids. The higher the affinity, the less pronounced was the blue shift and the larger was the fluorescence difference between free and bound peptide, a result indicating that the nature of the benzenesulfonamide spacer influenced the environmental change of the probe.

Benzenesulfonamides with oligoglycine substituents have been reported previously to bind less tightly to HCAII than those bearing alkyl groups,<sup>[26,28]</sup> a tendency that was also observed here. The affinity of KE2-D(15)-**6** was two orders of magnitude lower than that of KE2-D(15)-**5** although they had ligands with similar spacer lengths. As observed for the aliphatic benzenesulfonamides, the binding affinity of the peptide-associated glycine derivative was lower than that of a similar ligand not coupled to the polypeptide scaffold (Table 2).

The affinity of KE2-D(15)-**5** for HCAII (0.02  $\mu\text{M}$ ) was compared to that for the bovine equivalent BCAII (0.2  $\mu\text{M}$ ) as well as to that for the isozyme human carbonic anhydrase I (HCAI, 0.01 mM, Figure 4). Our results are in agreement with earlier studies of benzenesulfonamide interactions with HCAII<sup>[26]</sup> and BCAII<sup>[29]</sup> where tighter binding by the ligands to HCAII has been observed (Table 2). The dif-

ference between HCAI and HCAII in binding sulfonamides is ligand-dependent: HCAI binds dansylamide better than does HCAII,<sup>[37]</sup> but HCAII is superior in binding 2-acetylaminido-1,3,4-thiadiazole-5-sulfonamide (acetazolamide).<sup>[38,39]</sup>

Acetazolamide (8, Scheme 1)<sup>[40]</sup> is a nanomolar inhibitor of CA that has been exhaustively studied due to its

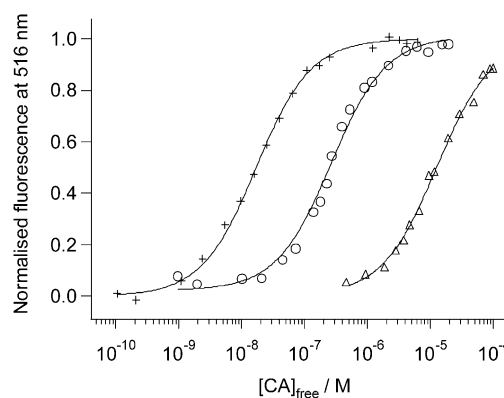


Figure 4. Titration of 1  $\mu\text{M}$  KE2-D(15)-**5** (or 0.8  $\mu\text{M}$  in the case of HCAII) with HCAII (+,  $K_d=0.02$   $\mu\text{M}$ ), BCAII ( $\circ$ , 0.2  $\mu\text{M}$ ) and HCAI ( $\triangle$ , 0.01 mM). The solid lines represent the best fit to the experimental data of an equation that describes the dissociation of a bimolecular complex. The measurements were performed in duplicate and representative curves are shown.

early recognition as an antiglaucoma drug. KE2-D(15)-**5** and HCAII were mixed in proportions where the degree of complex formation was at least 98%. When titrating the sample with acetazolamide, the fluorescence decreased as a consequence of the increasing concentration of free peptide due to efficient acetazolamide competition for the HCAII binding sites (Figure 5). Control experiments where the peptide was titrated with acetazolamide in the absence of HCAII revealed that the inhibitor itself caused some minor fluorescence quenching. Under the assumption that these two phenomena can be treated additively, the competition data was compensated for inhibitor quenching by correction with data from the control experiment. No photobleaching of the probe was observed during the titration process. The measurement was performed twice, with 2 and 4  $\mu\text{M}$  peptide, and the affinity of acetazolamide for HCAII was estimated to be 4 nM from both measurements. Literature values differ considerably, from 7–70 nM,<sup>[27,38,39,41]</sup> probably according to the method and conditions chosen for the affinity analysis. Apart from confirming that the fluorescence changes of KE2-D(15)-X upon titration with CA are due to binding of the benzenesulfonamide-linked peptide to the active site of the enzyme, this experiment highlights the possibility of screening substance libraries for new target-protein binders.

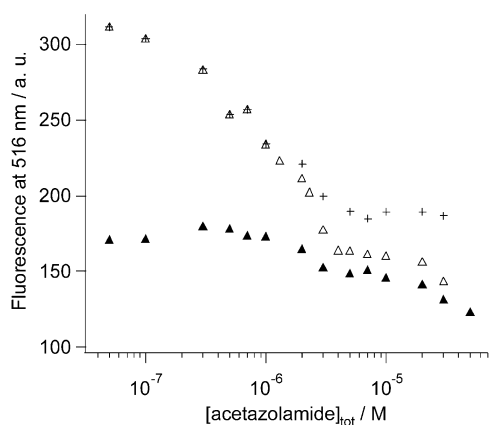


Figure 5. Competition for 1  $\mu\text{M}$  HCAII between 2  $\mu\text{M}$  KE2-D(15)-5 and acetazolamide ( $\Delta$ ). The observed quenching of the fluorescence of the dansyl probe with increased acetazolamide concentration was a result of the increasing concentration of free KE2-D(15)-5 as HCAII binding sites became occupied by acetazolamide. However, when the titration was carried out in the absence of HCAII ( $\blacktriangle$ ), some quenching was still observed for acetazolamide concentrations above 1  $\mu\text{M}$ . Fluorescence intensities recorded under titration conditions at  $[\text{acetazolamide}]_{\text{tot}} > 1 \mu\text{M}$  ( $\Delta$ ) were compensated by the addition of the difference between the average fluorescence intensities at  $[\text{acetazolamide}]_{\text{tot}} \leq 1 \mu\text{M}$  and each recorded intensity for which  $[\text{acetazolamide}]_{\text{tot}} > 1 \mu\text{M}$  ( $\blacktriangle$ ). The HCAII affinity for acetazolamide was estimated to be 4 nM, based on the corrected curve (+).

All fluorescence experiments were performed in a 2-[4-(2-hydroxyethyl)-1-piperazinyl]ethanesulfonic acid (HEPES) buffer containing a physiological concentration of NaCl (0.15 M). Most monovalent anions inhibit CA and  $\text{Cl}^-$  ions have a bovine CA binding constant of 0.19 M.<sup>[42]</sup> Although the concentration of  $\text{Cl}^-$  ions in the samples was comparable to this affinity, the presence of  $\text{Cl}^-$  ions only slightly affected the analysis due to the much tighter binding of the peptides. When data from measurements with the micromolar-affinity peptides KE2-D(15)-X (X=1–4, 6) were refitted with an equation allowing for two competing ligands, one of which had a  $K_d$  value of 0.19 M, the apparent affinities were increased by factors of 1.4–1.8. No measurable influence from the presence of  $\text{Cl}^-$  ions on the affinity of the nanomolar-affinity peptide KE2-D(15)-5 was expected. Addition of inhibitors of appropriate affinities in the sample may therefore be used for tuning the array by decreasing the apparent affinity of weak-binding array members while not affecting tight-binding ones.

## Discussion

The expression of parts of a proteome can be monitored by bioanalytical arrays of capture molecules such as antibodies, aptamers, affibodies, etc.<sup>[2]</sup> on chips or in microtitre-plate format. ELISA-like sandwich strategies or sample labelling, for example, by radioisotopes, are commonly applied for detection. An appealing alternative is a one-step analysis where the desired specific recognition is directly integrated with monitoring of target-protein binding. We propose a versatile molecular platform based on synthetic, folded helix–loop–helix polypeptides where recognition elements and flu-

orescent reporter groups are flexibly attached on the side chains of individually addressable lysine residues. Optimization of the capture element for a particular target protein is aided by the relative ease by which structures, interresidue distances and relative directionalities of the attached groups can be varied. This is a general advantage with choosing a large scaffold, although optimization of all the mentioned parameters may not always be necessary for the realization of a functional peptide. Synthetic polypeptides are attractive capture molecules as they are robust and easy to produce.

For target-protein quantification, an array of capture elements with different affinities for the analyte is an attractive alternative to traditional dilution techniques where the sample concentration must be systematically varied to match the affinities between analytes and capture molecules. The affinity of a functionalized, folded polypeptide for a target protein can be varied over several orders of magnitude and with relative ease in comparison with other scaffolds. The ligand can be modified by the incorporation of spacers capable of nonspecific interactions with the target. The affinity can also be varied by modification of the scaffold structure, through incorporation of amino acid residues or groups that enhance or decrease the affinity for the target due to electrostatic, hydrophobic or steric effects. To further expand the range of the array, a competing ligand of appropriate affinity can be added to the sample to decrease the apparent affinity, with weak-binding array members affected more than tight-binding ones.

In the design of an affinity array for CA, we varied the *para* substituents of the benzenesulfonamide ligand to provide spacers capable of modulating the interactions between the ligand and the CA binding pocket. We hypothesized that variation of the spacer structure would provide a range of binding affinities, but also that the bulky scaffold, which was not expected to fit into the binding pocket of the enzyme, would further modulate the interaction due to steric strain between target protein and the polypeptide; this would provide a general strategy for the design of affinity arrays. Following this general approach, six array members were synthesized and dissociation constants in the range  $10^{-8}$ – $10^{-6}$  M were obtained. Benzenesulfonamides with aliphatic *para* substituents have affinities for CA in the nanomolar range, because the affinity for the zinc ion in the active site is enhanced by interactions between the aliphatic substituent and a hydrophobic patch in the enzyme binding cleft. The binding strength is increased in a stepwise manner in proportion to the number of methylene groups.<sup>[26,29]</sup> When attached to the polypeptide scaffold, the affinities of array members bearing one, three and four methylene groups were found to be similar and approximately 1  $\mu\text{M}$ . This is most likely a result of steric interference that obscures the manifestation of the intrinsic and gradually increasing affinities of the ligands. However, the affinity dramatically increased by two orders of magnitude when five methylene groups were present in the spacer. The affinity difference between KE2-D(15)-4 and KE2-D(15)-5 may be due to a highly cooperative and optimal arrangement of multiple affinity-enhancing contributors such as the aliphatic spacer, the fluorescence probe or other residues of the scaffold.

fold. The affinity profile of benzenesulfonamides with aliphatic *para* substituents changing from stepwise to switch-like upon incorporation into the scaffold was an unexpected result, as switch-like affinity behavior is expected from a rigid rather than from a dynamic protein structure. Substantial flexibility of the protein and/or the polypeptide was, in fact, demonstrated by specific binding of the sulfonamide moiety attached to short-spaced ligands that, according to the crystal structure of HCAII in complex with a benzenesulfonamide inhibitor, should not be able to reach deep enough into the pocket without severe steric strain. The binding distance would be too long if the structures remained undistorted.<sup>[30]</sup> A possible explanation for the observed result may be that, if CA is distorted by the scaffold, the protein structure is no longer complementary to the preferred conformation of the spacer and the protein–ligand interactions that account for the observed nanomolar affinities of ligands not linked to the scaffold do not arise. With this interpretation, our findings indicate that minute changes induce dramatic structural effects in the protein at a critical spacer length. Nevertheless, the results demonstrate that a variation in spacer length and composition is a general approach to the design of affinity arrays.

Although five of the array members clustered at low micromolar affinity, the principle of HCAII-concentration determination in an unknown sample by using the affinity array can be illustrated (Figure 6). Data from Figure 3, obtained from measurements at a constant total concentration of HCAII, are presented as normalized fluorescence intensities of each of the array members plotted versus their affinities. With enough data points, the fitting of an equation describing the theoretical binding model (Equation (2) in the

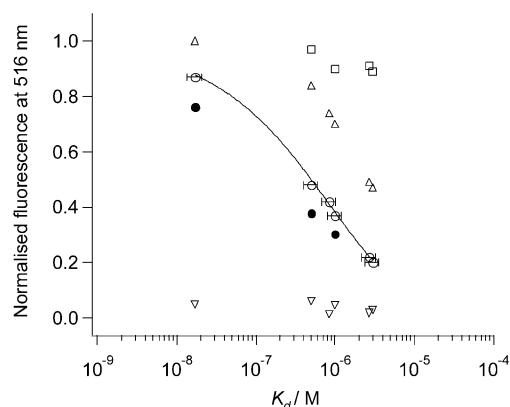


Figure 6. Normalized fluorescence intensities for different values of  $[HCAII]_{tot}$  plotted versus the  $K_d$  values of the KE2-D(15)-X (X=1–6) array (from Figure 3). Five different  $[HCAII]_{tot}$  values were chosen: 50 nM ( $\nabla$ ), 0.8  $\mu$ M ( $\bullet$ ), 1  $\mu$ M ( $\circ$ ), 3  $\mu$ M ( $\triangle$ ) and 30  $\mu$ M ( $\square$ ). Fluorescence data for KE2-D(15)-5 ( $K_d=0.02 \mu$ M) were collected at  $[KE2-D(15)-5]_{tot}=0.8 \mu$ M, but for comparison with the other peptides measured at 1  $\mu$ M it was corrected through subtraction of the theoretical difference between the signal at 0.8 and 1  $\mu$ M from the original experimental data. The estimated experimental error in the  $K_d$  values ( $\pm 20\%$ ) is indicated for  $[HCAII]_{tot}=1 \mu$ M.  $[HCAII]_{tot}=30 \mu$ M saturates the array, while 50 nM is too dilute to induce a response. The optimum concentration is in the low micromolar range, where data for 0.8 and 1  $\mu$ M can be resolved. The solid line is the theoretical binding curve for  $[HCAII]_{tot}=1 \mu$ M when the plateau values are set to 1 and 0.

Experimental Section) to the experimental results provides a direct readout of HCAII concentration, provided that the sample concentration matches the affinity range of the array and that start and end plateaus can be determined. The range of the array affinities should span at least three orders of magnitude, unless, instead of fitting, the fraction of peptide complexed by HCAII is estimated from the fluorescence-intensity change of individual array members upon complexation. As the peptide concentration is known, HCAII concentration can be readily determined with this strategy provided that calibrated intensities of fully complexed polypeptides are available. Optimal array performance, where the largest signal differences are obtained between array members, is obtained when the peptide concentration is less than the lowest  $K_d$  value and the protein concentration is close to the average of the highest and lowest  $K_d$  values. In Figure 6 the peptide concentration is suboptimally 1  $\mu$ M, which is close to the highest  $K_d$  value. Still, for HCAII concentrations in the micromolar range, concentration differences of 20–30% are detectable. The reliability of the analysis is directly related to the number of array members.

This discussion is of general applicability to the design of affinity arrays and illustrates the need for flexible and readily functionalized sensor platforms. The designed four-helix-bundle proteins reported here represent versatile scaffolds in which huge chemical diversity can be generated in a short time by procedures that are conveniently automated. Array members with widely different affinities and reporter properties are obtained with efforts that are modest in comparison with traditional approaches in organic chemistry and protein chemistry.

Designed proteins are not limited to use as scaffolds for affinity arrays but are also readily applied to several other related bioanalytical problems in biochemistry, diagnostics and pharmaceutical chemistry. Affinity screening of protein isoforms or mutants was demonstrated with KE2-D(15)-5 by discrimination between the three CA isozymes, HCAI, HCAII and BCAII. If the target protein is an enzyme and the ligand is a competitive inhibitor, the array also provides a means of estimating enzyme activity more conveniently than by traditional assays based on spectrophotometry. Diagnostic protein profiling could reveal differences between the patient and the control with respect to expression levels of different isoforms of the target protein. As a screening platform for pharmaceutical purposes, the array could be challenged with substance libraries to identify new ligands. The library-screening idea was demonstrated with the acetazolamide competition experiments, where the affinity of the competitive inhibitor was measured. This concept could also provide a route to new ligands for target proteins from combinatorial libraries in the case when no tight-binding ligands are known.

This work describes fundamental properties of a multifunctional capture element designed for a variety of biosensor and protein chip applications. Our approach applies to cases where the protein is known and at least one ligand is available or can be guessed. Incorporated into the scaffold, the known ligand may be the starting point for screening



substance libraries for better ligands. An affinity array can be designed by varying specific or nonspecific ligand–protein interactions that arise from variation of the ligand, the spacer or the scaffold. Depending on the interaction studied and on the application, issues of fluorophore and ligand array optimization, peptide immobilization or nonspecific binding of other proteins present in a blood sample or lysate may call for solutions. Finding these solutions will be facilitated by the flexibility of the polypeptide scaffold in terms of amino acid variation, as well as options for postsynthetic modifications.

## Conclusion

This work proposes the use of designed, functionalized polypeptides as efficient capture elements for protein detection and quantification in an analytical array format. The relative ease by which individually addressable lysine side chains may be functionalized facilitates optimization of the platform for the interaction system of interest, while integration of the processes of recognition and reporting allows one-step analyses of protein abundance, activity and affinity. For the model system of carbonic anhydrase and benzenesulfonamide, an affinity array was designed where, at a critical benzenesulfonamide spacer length, subtle spacer differences induced a profound effect on the affinity. Discrimination between different carbonic anhydrase isoforms and a concept for finding new ligands by competition studies was also demonstrated. These experiments are milestones on the way towards the design of a protein chip with immobilized capture polypeptides, where issues within biochemistry, diagnostics or pharmaceutical chemistry can be addressed.

## Experimental Section

The origin of chemicals obtained from standard chemical suppliers is not stated.

**Synthesis of benzenesulfonamide derivatives:** Active esters of inhibitors were prepared following procedures described previously for similar compounds,<sup>[28]</sup> with minor modifications. 4-Carboxybenzenesulfonamide was used as the starting material for all inhibitors. Yields were not optimized.

**H<sub>2</sub>NO<sub>2</sub>S(C<sub>6</sub>H<sub>4</sub>)CO<sub>2</sub>(NC<sub>4</sub>H<sub>9</sub>O<sub>2</sub>) (1):** 4-Carboxybenzenesulfonamide (2.0 g, 10 mmol) and *N*-hydroxysuccinimide (NHS, 1.14 g, 10 mmol) were dissolved in a mixture of dioxane (20 mL) and *N,N*-dimethylformamide (DMF, 8 mL) and the mixture was cooled in an ice bath. Dicyclohexylcarbodiimide (DCC, 2.0 g, 10 mmol) was added to the solution and the reaction mixture was stirred overnight at 5°C. *N,N*-dicyclohexylurea (DCU) was removed by filtration. The solvent was reduced to an oil and crystallization from 2-propanol and hexane afforded a white solid (2.1 g, 73%); <sup>1</sup>H NMR (300 MHz, D<sub>2</sub>O, 25°C): δ = 8.35 (d, 2H), 8.11 (d, 2H), 3.03 (s, 4H) ppm.

**General procedure for the synthesis of H<sub>2</sub>NO<sub>2</sub>S(C<sub>6</sub>H<sub>4</sub>)CONH(CH<sub>2</sub>)<sub>*n*</sub>CO<sub>2</sub>(NC<sub>4</sub>H<sub>9</sub>O<sub>2</sub>) (2–5; *n* = 1, 3, 4, 5) and H<sub>2</sub>NO<sub>2</sub>S(C<sub>6</sub>H<sub>4</sub>)CO(Gly)<sub>3</sub>(NC<sub>4</sub>H<sub>9</sub>O<sub>2</sub>) (6):** 0.3 M Nucleophile (Gly, 4-aminobutyric acid, 5-aminopentanoic acid, 6-aminohexanoic acid or the tripeptide glycyl–glycyl–glycine, respectively, 1 equiv) in 50 mM sodium borate was added to 0.2 M **1** in acetone at pH 8.5. The reaction mixture was stirred at room temperature for at least two hours while the pH value was kept between 7.0 and 7.5 with 0.1 M NaOH. The reaction can be monitored by thin-layer chromatography by observing the disappearance of unreacted **1** (toluene:ethyl acetate

(1:3) with 4% acetic acid, *R<sub>f</sub>* = 0.6). The solution was acidified to pH 3 and reduced in vacuo. The intermediate carboxylic acid product, H<sub>2</sub>NO<sub>2</sub>S(C<sub>6</sub>H<sub>4</sub>)CONH(CH<sub>2</sub>)<sub>*n*</sub>COOH (*n* = 1, 3, 4, 5) or H<sub>2</sub>NO<sub>2</sub>S(C<sub>6</sub>H<sub>4</sub>)CO(Gly)<sub>3</sub>, was washed in cold water and dried. Yields were 62–79% and the purity was confirmed by <sup>1</sup>H NMR spectroscopy. To prepare the NHS ester, the intermediate product (1 equiv) was added to 0.1 M NHS (1.1 equiv) in dioxane:DMF (1:1) at 0°C. DCC (1 equiv) was added to the solution and the reaction mixture was stirred overnight at 5°C. DCU was removed by filtration. The solvent was reduced and a white solid (**2–6**) was precipitated from 2-propanol and hexane. The purity was confirmed by <sup>1</sup>H NMR spectroscopy and the yields were 36–66%. A typical synthetic procedure is provided below.

**H<sub>2</sub>NO<sub>2</sub>S(C<sub>6</sub>H<sub>4</sub>)CONH(CH<sub>2</sub>)<sub>5</sub>CO<sub>2</sub>(NC<sub>4</sub>H<sub>9</sub>O<sub>2</sub>) (5):** 6-Aminohexanoic acid (88 mg, 0.67 mmol) in 50 mM sodium borate (2 mL) was added to **1** (200 mg, 0.67 mmol) in acetone (3 mL) at pH 8.5. The reaction mixture was stirred at room temperature for two hours while keeping the pH value between 7.0 and 7.5, after which the solution was acidified to pH 3 and concentrated. The intermediate product H<sub>2</sub>NO<sub>2</sub>S(C<sub>6</sub>H<sub>4</sub>)CONH(CH<sub>2</sub>)<sub>5</sub>COOH was washed in cold water and vacuum dried to give a white solid (145 mg, 69%); <sup>1</sup>H NMR (300 MHz, D<sub>2</sub>O, 25°C): δ = 8.01 (d, 2H), 7.91 (d, 2H), 3.37 (t, 2H), 2.17 (t, 2H), 1.58 (m, 4H), 1.36 (m, 2H) ppm. H<sub>2</sub>NO<sub>2</sub>S(C<sub>6</sub>H<sub>4</sub>)CONH(CH<sub>2</sub>)<sub>5</sub>COOH (100 mg, 320 μmol) and NHS (41 mg, 352 μmol) were dissolved in a mixture of dioxane (1 mL) and DMF (1 mL) and the mixture was cooled in an ice bath. DCC (65 mg, 320 μmol) was added to the solution and the mixture was stirred overnight at 5°C. DCU was removed by filtration. The solvent was reduced to an oil and a white solid was precipitated from 2-propanol and hexane. Recrystallization from hot 2-propanol afforded the desired product (**5**, 47 mg, 36%); <sup>1</sup>H NMR (300 MHz, [D<sub>6</sub>]acetone, 25°C): δ = 8.02 (d, 2H), 7.95 (d, 2H), 7.87 (s, 1H), 6.66 (s, 2H), 3.44 (q, 2H), 2.88 (s, 4H), 2.66 (t, 2H), 1.78 (m, 2H), 1.69 (m, 2H), 1.54 (m, 2H) ppm.

**Peptide synthesis, purification and modification:** The polypeptide KE2 was synthesized on a Pioneer automated peptide synthesizer (Applied Biosystems) by using standard 9-fluorenylmethoxycarbonyl (Fmoc) chemistry. The synthesis was performed on a 0.2-mmol scale and an Fmoc-Gly–polyethylene glycol–polystyrene polymer (Applied Biosystems) with a substitution level of 0.18 mmol g<sup>-1</sup> was used. This resin was purchased with the first amino acid attached and the free acid was formed at the C terminus upon cleavage in trifluoroacetic acid (TFA). The side chains of the amino acids (Calbiochem–Novabiochem AG) were protected by base-stable groups: *tert*-butyl ester (Asp, Glu), *tert*-butoxymethyl (Lys), trityl (His, Asn, Gln) and 2,2,4,6,7-pentamethyl-2H-benzofuran-5-sulfonyl (Arg). To allow site-selective incorporation of a fluorescent probe at position 15, the side chain of Lys15 was protected by an allyloxycarbonyl (Applied Biosystems) group that can be selectively removed by treatment with tetrakis(triphenylphosphine)palladium(0). The Fmoc protecting groups were removed from the amino termini by treatment with 20% piperidine in DMF. A fourfold excess of amino acid was used in each coupling and amino acids were activated with a mixture of *O*-(7-benzotriazole-1-yl)-1,1,3,3-tetramethyluronium tetrafluoroborate (TBTU, 0.5 M in DMF; Alexis Biochemicals) and diisopropylethylamine (DIPEA, 1 M in DMF). A standard amino acid coupling time of 60 min was used, except in the cases of Gln and His (90 min) and Asn and Arg (120 min). The N terminus of the peptide was capped with 0.3 M acetic anhydride in DMF. After the completed synthesis, the resin was rinsed with dichloromethane (DCM) and dried in vacuo.

Before cleaving the peptide from the resin, Lys15 was deprotected over 3 h at room temperature by using [Pd(PPh<sub>3</sub>)<sub>4</sub>] (3 equiv) in a mixture of trichloromethane, acetic acid and *N*-methylmorpholine (17:2:1 v/v; 12 mL per g of polymer). The resin was washed sequentially with 20 mM diethyldithiocarbamic acid in DMF, 30 mM DIPEA in DMF, DMF and DCM, and then desiccated. For probe coupling, the resin was mixed with dansyl chloride (2 equiv) and DIPEA (7 equiv) in DMF (6 mL per g of polymer) and the mixture was left to stand with occasional swirling for 4 h at room temperature. The resin was washed with DMF and DCM and then desiccated. The dansylated peptide was cleaved from the resin by treatment with a mixture of TFA, triisopropylsilane, and water (95:2.5:2.5 v/v; 15 mL per g of polymer) over 2 h at room temperature. After filtration, the TFA was evaporated and the peptide was precipitated by addition of cold diethyl ether, centrifuged, washed in diethyl ether and lyophilized. The crude product was purified by reversed-phase

HPLC on a semipreparative HICROM C-8 column, eluted isocratically with 40% 2-propanol and 0.1% TFA in water at a flow rate of 10 mL min<sup>-1</sup>. The purified peptide was identified by MALDI-TOF mass spectrometry.

Benzenesulfonamides **1–6** (1.3 equiv) were added to 1 mM peptide solutions (prepared from lyophilized peptide under the assumption that it contains 25% water) in 50 mM Tris buffer (pH 8.0) to create the six-membered peptide array. The incorporation reaction was monitored by MALDI-TOF mass spectrometry. After one day at room temperature the reaction mixtures of peptides modified with **1–5** were purified by reversed-phase HPLC on a semipreparative HICROM C-8 column, eluted isocratically with 40% 2-propanol and 0.1% TFA in water at a flow rate of 10 mL min<sup>-1</sup>. The peptide modified with **6** was purified in the same way, except that a gradient of 30–70% acetonitrile and 0.1% TFA in water was applied over 60 min. Monomodification yields were 44–63%, while 10% dimodification (Lys33, Lys34) was observed.

**Concentration determination of proteins and peptides:** HCAI, HCAII and BCAII were obtained from Sigma and were used without further purification. The same protein batches were used for all experiments. Protein concentrations were determined from the absorbance at 280 nm by using extinction coefficients of 46800 (HCAI), 54800 (HCAII) and 55100 M<sup>-1</sup> cm<sup>-1</sup> (BCAII).<sup>[43]</sup> Concentrations of peptide stock solutions diluted 1:10 in methanol were determined from the absorbance at 335 nm by using an extinction coefficient of 4200 M<sup>-1</sup> cm<sup>-1</sup> (dansyl)<sup>[35]</sup> and were subsequently confirmed by amino acid analysis (Aminosyraanalyscentralen, Uppsala, Sweden).

**Structure determination with circular dichroism spectroscopy:** Circular dichroism spectra were recorded on a CD6 spectrodichograph (Jobin-Yvon Instruments SA) by using a 10-mm cuvette in the interval 260–203 nm at room temperature. Spectra of 1 μM (or 0.8 μM in the case of KE2-D(15)-5) peptide in 100 mM sodium phosphate at pH 7.4 were obtained by collecting data at 0.5 nm intervals with an integration time of 1 s. Each spectrum was collected as an average of three scans and the data were corrected by subtraction of a spectrum of a blank sample containing only buffer. The helical content was determined as the mean residue ellipticity at 222 nm,  $[\theta]_{222}$ , and was calculated from Equation (1), where  $\theta_{222}^{\text{obs}}$  is the observed ellipticity at 222 nm (deg),  $mrw$  is the mean residue weight (g mol<sup>-1</sup>),  $c$  is the peptide concentration (g mL<sup>-1</sup>) and  $l$  is the optical path length of the cell (cm).

$$[\theta]_{222} = \frac{\theta_{222}^{\text{obs}} mrw}{10lc} \quad (1)$$

**Affinity determination with fluorescence spectroscopy:** Fluorescence spectra were recorded on a F-4500 spectrofluorophotometer (Hitachi High-Technologies Corp.) by using a 10-mm quartz cuvette at 23°C. The excitation wavelength was 335 nm and the emission was monitored in the range 450–650 nm. Excitation and emission slits were 5 nm. Each spectrum represents an average of two scans. For affinity determinations, samples of 1 μM (or 0.8 μM in the case of KE2-D(15)-5) peptide in HEPES-buffered saline (10 mM HEPES, 150 mM NaCl, pH 7.4; Biacore AB) were titrated with solutions of 1, 10 and 100 μM CA (HCAI, HCAII or BCAII) diluted from a stock solution of 500 μM CA in HEPES-buffered saline. The fluorescence intensity at 516 nm was monitored as a function of the total protein concentration and the dissociation constant  $K_d$  was determined by fitting Equation (2) to the experimental results under the assumption of a 1:1 binding model.

$$F_{\text{obs}} = \frac{F_{\text{bound}}[\text{CA}] + F_{\text{free}}K_d}{[\text{CA}] + K_d} \quad (2)$$

In Equation (2),  $F_{\text{obs}}$  is the observed fluorescence intensity,  $F_{\text{bound}}$  is the fluorescence of the peptide bound to CA,  $F_{\text{free}}$  is the fluorescence of the free peptide and  $[\text{CA}]$  is the concentration of free CA.  $[\text{CA}]$  can be derived from Equation (3), where  $[\text{P}]_{\text{tot}}$  is the total concentration of peptide and  $[\text{CA}]_{\text{tot}}$  is the total concentration of CA.

$$[\text{CA}] = -\frac{[\text{P}]_{\text{tot}} + K_d - [\text{CA}]_{\text{tot}}}{2} + \sqrt{\left(\frac{[\text{P}]_{\text{tot}} + K_d - [\text{CA}]_{\text{tot}}}{2}\right)^2 + K_d[\text{CA}]_{\text{tot}}} \quad (3)$$

Fitting was done with IGOR Pro 4.03 software (WaveMetrics Inc.). For estimation of the influence of Cl<sup>-</sup> ions on the measured affinities, Equation (2) was used with the expression for  $[\text{CA}]$  given in Equation (4), where  $[\text{Cl}^-]_{\text{tot}}$  is the total concentration of chloride ions,  $[\text{CAP}]$  is the concentration of CA complexed by the peptide and  $K_{\text{Cl}}$  is the affinity constant of chloride-ion binding to CA.  $[\text{CAP}]$  was estimated from the experimental data.

$$[\text{CA}] = \frac{[\text{CA}]_{\text{tot}} - [\text{CAP}] - [\text{Cl}^-]_{\text{tot}} - K_{\text{Cl}}}{2} + \sqrt{\left(\frac{[\text{CA}]_{\text{tot}} - [\text{CAP}] - [\text{Cl}^-]_{\text{tot}} - K_{\text{Cl}}}{2}\right)^2 + K_{\text{Cl}}([\text{CA}]_{\text{tot}} - [\text{CAP]})} \quad (4)$$

**Competition experiments with acetazolamide:** Mixtures of 1 μM HCAII and 2 μM E2-D(15)-5 or 1 μM HCAII and 4 μM KE2-D(15)-5 in HEPES-buffered saline (10 mM HEPES, 150 mM NaCl, pH 7.4; Biacore AB) were titrated with solutions of 10 and 100 μM acetazolamide. The excitation wavelength was 335 nm and the emission was monitored in the range 450–650 nm. Excitation and emission slits were 5 nm. Each spectrum represents an average of two scans. Control experiments were performed where 2 or 4 μM peptide was titrated with acetazolamide in the absence of protein. The dissociation constant  $K_i$  of the interaction between KE2-D(15)-5 and acetazolamide was estimated from the total acetazolamide concentration  $[\text{A}]_{\text{tot}}$  at which the fluorescence was intermediate between its maximum and minimum values, that is, where the concentration of peptide-bound HCAII equals the concentration of acetazolamide-bound HCAII. At this point, provided the concentration of free protein is neglected, Equation (5) is applicable, where  $K_d$  is the dissociation constant of the peptide–protein complex and  $[\text{P}]_{\text{tot}}$  is the total peptide concentration.

$$K_i = K_d \frac{[\text{A}]_{\text{tot}} - \frac{[\text{HCAII}]_{\text{tot}}}{2}}{[\text{P}]_{\text{tot}} - \frac{[\text{HCAII}]_{\text{tot}}}{2}} \quad (5)$$

## Acknowledgments

K.E. is enrolled in the graduate school Forum Scientium and in the research program Biomimetic Materials Science, both financed by the Swedish Foundation for Strategic Research (SSF). Financial support from the Swedish Research Council (VR) is also gratefully acknowledged.

- [1] T. Kodadek, *Chem. Biol.* **2001**, *8*, 105.
- [2] M. F. Templin, D. Stoll, M. Schrenk, P. C. Traub, C. F. Vohringer, T. O. Joos, *Trends Biotechnol.* **2002**, *20*, 160.
- [3] H. Zhu, M. Snyder, *Curr. Opin. Chem. Biol.* **2003**, *7*, 55.
- [4] L. Bracci, L. Lozzi, B. Lelli, A. Pini, P. Neri, *Biochemistry* **2001**, *40*, 6611.
- [5] F. Toepert, J. R. Pires, C. Landgraf, H. Oschkinat, J. Schneider-Mergener, *Angew. Chem.* **2001**, *113*, 922; *Angew. Chem. Int. Ed.* **2001**, *40*, 897.
- [6] B. T. Houseman, J. H. Huh, S. J. Kron, M. Mrksich, *Nat. Biotechnol.* **2002**, *20*, 270.
- [7] M. Takahashi, K. Nokihara, H. Mihara, *Chem. Biol.* **2003**, *10*, 53.
- [8] J. L. Naffin, Y. Han, H. J. Olivos, M. M. Reddy, T. Sun, T. Kodadek, *Chem. Biol.* **2003**, *10*, 251.
- [9] A. Q. Emili, G. Cagney, *Nat. Biotechnol.* **2000**, *18*, 393.
- [10] K. Broo, L. Brive, A. C. Lundh, P. Ahlberg, L. Baltzer, *J. Am. Chem. Soc.* **1996**, *118*, 8172.
- [11] L. K. Andersson, G. T. Dolphin, L. Baltzer, *ChemBioChem* **2002**, *3*, 741.
- [12] L. K. Andersson, M. Caspersson, L. Baltzer, *Chem. Eur. J.* **2002**, *8*, 3687.
- [13] L. K. Andersson, G. Stenhagen, L. Baltzer, *J. Org. Chem.* **1998**, *63*, 1366.
- [14] S. Vijayalekshmi, S. K. George, L. K. Andersson, J. Kihlberg, L. Baltzer, *Org. Biomol. Chem.* **2003**, *1*, 2455.
- [15] K. Enander, G. T. Dolphin, L. K. Andersson, B. Liedberg, I. Lundström, L. Baltzer, *J. Org. Chem.* **2002**, *67*, 3120.

- [16] D. R. Thevenot, K. Toth, R. A. Durst, G. S. Wilson, *Pure Appl. Chem.* **1999**, *71*, 2333.
- [17] H. W. Hellinga, J. S. Marvin, *Trends Biotechnol.* **1998**, *16*, 183.
- [18] S. Olofsson, G. Johansson, L. Baltzer, *J. Chem. Soc. Perkin Trans. 2* **1995**, 2047.
- [19] S. Olofsson, L. Baltzer, *Folding Des.* **1996**, *1*, 347.
- [20] L. K. Andersson, PhD thesis, Göteborg University, Sweden, **2001**.
- [21] A. Liljas, K. Håkansson, B.-H. Jonsson, Y. F. Xue, *Eur. J. Biochem.* **1994**, *219*, 1.
- [22] T. Mann, D. Keilin, *Nature* **1940**, *146*, 164.
- [23] H. A. Krebs, *Biochem. J.* **1948**, *43*, 525.
- [24] S. Lindskog, P. J. Wistrand in *Design of Enzyme Inhibitors as Drugs* (Eds.: M. Sandler, H. J. Smith), Oxford University Press, Oxford, **1988**.
- [25] P. W. Taylor, R. W. King, A. S. V. Burgen, *Biochemistry* **1970**, *9*, 2638.
- [26] R. W. King, A. S. V. Burgen, *Proc. R. Soc. London Ser. B* **1976**, *193*, 107.
- [27] A. Jain, G. M. Whitesides, R. S. Alexander, D. W. Christianson, *J. Med. Chem.* **1994**, *37*, 2100.
- [28] A. Jain, S. G. Huang, G. M. Whitesides, *J. Am. Chem. Soc.* **1994**, *116*, 5057.
- [29] J. M. Gao, S. Qiao, G. M. Whitesides, *J. Med. Chem.* **1995**, *38*, 2292.
- [30] P. A. Boriack, D. W. Christianson, J. Kingerywood, G. M. Whitesides, *J. Med. Chem.* **1995**, *38*, 2286.
- [31] G. B. Sigal, G. M. Whitesides, *Bioorg. Med. Chem. Lett.* **1996**, *6*, 559.
- [32] A. E. Eriksson, P. M. Kylsten, T. A. Jones, A. Liljas, *Proteins* **1988**, *4*, 283.
- [33] G. Weber, *Biochem. J.* **1952**, *51*, 155.
- [34] J. R. Lakowicz, *Principles of Fluorescence Spectroscopy*, Kluwer Academic/Plenum Publishers, New York, **1999**.
- [35] R. P. Haugland, *Molecular Probes: Handbook of Fluorescent Probes and Research Chemicals*, to be found under <http://www.probes.com/handbook>, **2003**.
- [36] L. K. Andersson, G. T. Dolphin, J. Kihlberg, L. Baltzer, *J. Chem. Soc. Perkin Trans. 2* **2000**, 459.
- [37] C. Engstrand, B. H. Jonsson, S. Lindskog, *Eur. J. Biochem.* **1995**, *229*, 696.
- [38] O. Arslan, O. I. Kufrevioglu, B. Nalbantoglu, *Bioorg. Med. Chem.* **1997**, *5*, 515.
- [39] C. T. Supuran, A. Scozzafava, *J. Enzyme Inhib.* **2000**, *15*, 597.
- [40] J. O. J. Roblin, J. W. Clapp, *J. Am. Chem. Soc.* **1950**, *72*, 4890.
- [41] T. H. Maren in *The Carbonic Anhydrases: New Horizons* (Eds.: W. R. Chegwidden, N. D. Carter, Y. H. Edwards), Birkhäuser Verlag, Basel, **2000**.
- [42] Y. Pocker, J. T. Stone, *Biochemistry* **1968**, *7*, 2936.
- [43] S. Lindskog, L. E. Henderson, K. K. Kannan, A. Liljas, P. O. Nyman, B. Strandberg in *The Enzymes, Vol 5* (Ed.: P. D. Boyer), Academic Press, New York, **1971**.
- [44] A. Fersht, *Structure and Mechanism in Protein Science: A Guide to Enzyme Catalysis and Protein Folding*, W. H. Freeman, New York, **1999**.
- [45] D. W. Banner, M. Kokkinidis, D. Tsernoglou, *J. Mol. Biol.* **1987**, *196*, 657.

Received: July 26, 2003

Revised: January 5, 2004 [F5391]

Published online: April 15, 2004